J Mol Model (2011) 17:1413–1425
DOI 10.1007/s00894-010-0839-9

ORIGINAL PAPER

A comparative study of one- and two-photon absorption properties of pyrene and perylene diimide derivatives

Xiao-Ting Liu · Yang Zhao · Ai-Min Ren · Ji-Kang Feng

Received: 7 June 2010 / Accepted: 25 August 2010 / Published online: 16 September 2010

Abstract Two important classes of organic molecules, perylene diimide (PDI) and pyrene derivatives have been found to possess relatively excellent photophysical and photochemical properties and especially high two-photon absorption cross sections (δ^{T}_{max}). Herein, one-photon absorption (OPA) and two-photon absorption (TPA) properties of some novel PDI and pyrene derivatives were comparatively investigated by the density functional theory (DFT) and Zerner's intermediate neglect of differential overlap (ZINDO) methods. The calculated results indicate that with respect to PDI derivatives, the maximum TPA cross-sections for pyrene compounds increase obviously, the maximum peaks of OPA and TPA spectra are blue-shifted, the $\Delta E_{H\text{-}L}$ (energy gaps between the highest occupied orbital and the lowest unoccupied orbital) increase. The different π-conjugated bridges (fluorene and pyrene) and terminal groups have slight effect on the OPA properties. Nevertheless, the molecules bearing 1,6-disubstituted pyrene as the π-conjugated bridge display the largest δ^{T}_{max} in both series of compounds **3** and **4**. Moreover, the δ^{T}_{max} values of molecules with benzothiazole-substituted terminal groups are larger than those of the molecules with diphenylamine, which is attributed to benzothiazole groups stabilizing the planarity of the branch parts, extending the conjugated length and increasing the π-electron delocalized extent. Furthermore, the molecular size has marked effect on OPA and TPA properties. It is worthy to mention that cruciform **8** displays the largest δ^{T}_{max} among all the studied molecules in the range of 600–1100 nm. This research could provide a better understanding for the origin of the linear and nonlinear optical properties, and it would be helpful to gain more information about designing two-photon absorption materials with large δ^{T}_{max}.

Keywords Density functional theory · Electronic structure · Optical properties · Perylene diimide derivatives · Pyrene · Two-photon absorption

Electronic supplementary material The online version of this article (doi:10.1007/s00894-010-0839-9) contains supplementary material, which is available to authorized users.

X.-T. Liu · Y. Zhao · A.-M. Ren (✉) · J.-K. Feng
State Key Laboratory of Theoretical and Computational Chemistry, Institute of Theoretical Chemistry, Jilin University, Changchun 130023, People's Republic of China
e-mail: aimin_ren@yahoo.com

Introduction

Two-photon absorption (TPA) is defined as the electronic excitation of a molecule induced by a simultaneous absorption of a pair of photons with the same or different energy. Since this phenomenon was first predicted theoretically in 1931 [1] and demonstrated experimentally in 1961 [2], it has been the subject of intense scientific investigation. At present, many experimental and theoretical investigations have focused on seeking good TPA materials with larger TPA cross sections. A lot of progress has already been made and some materials have been widely used in microscopy [3, 4], microfabrication [5], three-dimensional data-storage [6–8], optical power limiting [9, 10], up-converted lasing [11], photodynamic therapy [12, 13] and others. With the increasing applications, the demands for novel desirable materials become urgent. This has stimulated the investigation of a variety of new chromophoric systems ranging from the well-known push-pull dipolar to quadrupolar, octupolar, multipolar and branched structures.

As an important class of organic chromophores, perylene diimide (PDI) derivatives have been found to possess relatively excellent photophysical and photochemical prop-

erties, and especially high TPA cross sections, which suggest their utility in a number of applications such as solar cells [14], fluorescent probes [15, 16], electron-transport materials [17, 18], sensitizers for photovoltaics [19], and two-photon absorbing dyes [20–23]. Therefore the design of PDI derivatives has attracted increasing interest in recent years by introducing appropriate structural modification. Belfield et al. [24, 25] have synthesized 2,9-bis(7-diphenylamino-9,9-didecylfluoren-2-yl)perylene diimide and 2,9-bis(7-benzothiazole-9,9-didecylfluoren-2-yl) perylene diimide and investigated their TPA properties by two-photon induced fluorescence and open aperture Z-scan methods under femtosecond and picosecond excitation, respectively. The results indicate that these two PDI derivatives have high TPA cross sections, and are applicable for optical power limiting and data storage. It has also been reported that the linear-optical property of PDI compounds is not very sensitive to the structure of terminal groups but mainly determined by the PDI center [25–27].

Pyrene has the superordinary planar π-conjugated configuration and stable electronic properties. Its derivatives have attracted considerable attention in various areas of chemical, environmental, and biological science as a fluorophore in recent years [28–31]. As two-photon absorption materials, several compounds firstly utilizing pyrene as the π-center have been synthesized and studied [32]. The results suggest that pyrene derivatives are efficient TPA materials due to their large TPA cross-sections, besides high fluorescent quantum yields.

To the best of our knowledge, up to now, there has been no comparative study on TPA properties between PDI and pyrene derivatives. A detailed comparative investigation on their TPA properties is necessary for designing practicable two-photon materials with larger TPA cross sections. In this work, based on two fluorenylperylene diimide compounds **1** and **2** [25] by replacing the π-bridge (fluorene) or center (perylene diimide) with pyrene and changing different substituent positions on the pyrene, some new compounds were designed, and their equilibrium geometries, electronic structures, OPA and TPA properties were theoretically discussed in detail. The purpose is to study the effect of the nature of center moieties, the character of π-conjugated bridges, the number of substituents and the nature of terminal groups with electron-acceptor (benzothiazolyl) or -donator (diphylamine) on one- and two-photon absorption properties. We hope our design would provide a useful guideline to experimental synthesis.

Computational methods

In this study, the geometrical structures of all molecules were fully optimized without any constraints by using the density functional theory (DFT) with the 6-31G(d) basis set and the B3LYP hybrid functional [33–35]. The geometry optimizations were confirmed by the frequency calculations. Following each optimization, the vibrational frequencies are all positive. Geometry optimizations and vibrational frequency calculations were performed by using Gaussian 03 program suite [36]. On the basis of the optimized structures, the computations of the electronic spectra were carried out by the time-dependent density functional theory (TDDFT) at the same level. In addition, the effect of solvent was taken into account within the self-consistent reaction field (SCRF) theory by using the polarized continuum model (PCM) approach [37–40]. The OPA properties of all the investigated molecules were also calculated by employing the Zerner's intermediate neglect of differential overlap (ZINDO) program including single and double electronic excitation configuration interaction.

The TPA process corresponds to simultaneous absorption of two photons. The TPA efficiency of an organic molecule, at optical frequency $\omega/2\pi$, can be characterized by the TPA cross-section $\delta(\omega)$. It can be directly related to the imaginary part of the third-order polarizability $\gamma(-\omega;\omega,\omega,\omega)$ by [41, 42]:

$$\delta(\omega) = \frac{3\hbar\omega^2}{2n^2c^2\varepsilon_0} L^4 \mathrm{Im}[\gamma(-\omega;\omega,-\omega,\omega)] \quad (1)$$

in which $\gamma(-\omega;\omega,\omega,\omega)$ is the third-order polarizability, $\hbar\omega$ is the energy of incoming photons, c is the speed of light, ε_0 is the vacuum electric permittivity, n denotes the refractive index of medium and L corresponds to the local-field factor. In the calculations presented here, n and L are set to 1 because of isolated molecule in vacuum.

The sum-over-states (SOS) expression to evaluate the components of the second hyperpolarizability $\gamma_{\alpha\beta\gamma\delta}$($\alpha$, β, γ, and δ refer to the molecular axes) can be deduced using perturbation theory. By considering a Taylor expansion of energy with respect to the applied field, the Cartesian components $\gamma_{\alpha\beta\gamma\delta}$ are given by Ref. [43] and [44].

To compare the calculated δ value with the experimental value measured in solution, the damping factor (Γ_K) of excited state K in the SOS expression is set to 0.1 eV [45, 46]. And the orientationally averaged (isotropic) value of γ is evaluated, which is defined as

$$\langle\gamma\rangle = \frac{1}{15}\sum_{i,j}\left(\gamma_{iijj} + \gamma_{ijij} + \gamma_{ijji}\right) \quad i,j = x,y,z. \quad (2)$$

Taking the imaginary part of $<\gamma>$ value into the expression (1), $\delta(\omega)$ can be obtained in comparison with the experimental value.

In principle, any kind of self-consistent-field molecular orbital procedure combined with the configuration interaction (CI) can be used to calculate the physical values in the

above expression. In this work, the properties of electronic excited states were obtained by single and double electronic excitation configuration interaction (SDCI) using ZINDO program. Moreover, the transition energies and transition moments were also obtained by ZINDO calculation. Then, the FTRNLO program compiled by our group was used to calculate the second hyperpolarizability γ and two-photon absorption cross section $\delta(\omega)$. The calculated TPA cross-sections of all molecules included the contributions from 300 lowest-lying excited states. In order to ascertain whether 300 states were sufficient for the convergence of $\delta(\omega)$, we chose the largest molecule **7** as an example to consider sum-over-states truncation. As shown in Fig. 1, when the number of states reaches 250 states, calculated $\delta(\omega)$ has already been converged. Hence, a chosen number of 300 states included in the SOS expansion was sufficient for the convergence of $\delta(\omega)$ of all molecules in this paper.

Results and discussions

Molecular design and geometry optimization

The molecular structures of all compounds are represented in Fig. 2. The construction of the series of quadrupolar chromophores **3**, **4**, **5**, **6**, **7** and **8** was based on compounds **1** and **2** [25]. Besides, the decyl groups of the fluorenes for compounds **1** and **2** were all replaced by methyl groups during the calculations. By replacing the fluorene π-bridge with pyrene and changing different substituent positions (1,6-, 1,8-, and 2,7-) of pyrene, we designed PDI derivatives **3-1**, **3-2**, **3-3** and **4-1**, **4-2**, **4-3**. The study of the two series of molecules can allow us to ascertain the effect of the π-conjugated bridges and electron-donating or -accepting terminal groups on OPA and TPA properties.

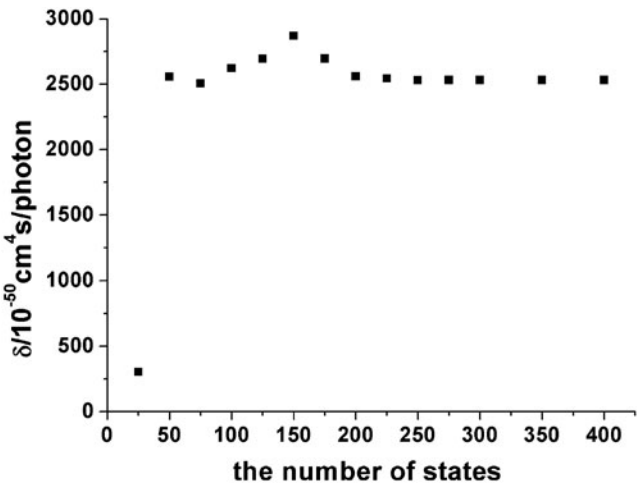

Fig. 1 Relationship of ZINDO-derived δ^{T}_{max} and the number of states for compound **7**

And then we built two other series of molecules **5-1**, **5-2**, **5-3** and **6-1**, **6-2**, **6-3** through changing the PDI center for the pyrene core and containing the lateral side groups. It has been reported that the cruciforms exhibiting the high degree of conjugation and multiple pathways for intramolecular charger-transfer (ICT) have potential for the enhancement of TPA cross sections [47]. With this in mind, molecules **7** and **8** were studied where four fluorenyl terminal groups are connected via a pyrene core. The difference between series of molecules **1**, **3**, **5**, **7** and **2**, **4**, **6**, **8** is terminal groups with electron-accepting (benzothiazole) or -donating (diphenylamine) substituents. The structural motif of all studied molecules is the D-π-A-π-D or A-π-D-π-A (D = donor, A = acceptor) type.

The optimized ground state geometries of all molecules in this work are stable and the first vibrational frequency shows positive. Their lowest energies (a.u.) are shown in Fig. S1. It can be seen that the cores of all PDI derivatives remain planar and the PDI body is almost perpendicular to the π-bridge planes (fluorene plane or pyrene plane). For instance, the dihedral angles between the central moiety and π-bridge planes of molecules **1**, **2**, **3-1**, **4-2**, and **4-3** are 93°, 90°, 90°, 90°, and 91°, respectively. But for pyrene derivatives **5-1**, **5-2**, and **5-3**, the dihedral angles are 141°, 126°, and 128°, respectively. For compounds **6-1**, **6-2**, and **6-3**, the values are the same as **5-1**, **5-2**, and **5-3**, respectively. And the dihedral angles between the pyrene body and each branch of molecules **7** and **8** range from 123° to 128°. The benzothiazole plane of all molecules is nearly coplanar with the π-bridge planes, except for molecules **4-2** and **4-3**. For them, the benzothiazole substituents on the pyrene are twisted by about 29° and 42°, respectively (see Fig. S1). This distortion of geometry is due to the steric effect. In addition, both the *trans*- and *cis*-isomers of molecules **1** and **2** were optimized considering that the centrosymmetric and noncentrosymmetric molecules obey different selection rules for two-photon absorption. The optimized results show that the energies of two isomers are quite similar (see Fig. S1).

Electronic structures

Electronic structures are fundamental for understanding electronic absorption spectra. The calculated frontier orbital energies (four occupied orbitals, four unoccupied orbitals and energy gap ($\Delta E_{H\text{-}L}$) between the highest occupied molecular orbital (HOMO) and the lowest unoccupied molecular orbital (LUMO)) are shown in Fig. 3. As can be seen, the LUMO energies of PDI and pyrene compounds are the dominating factor in $\Delta E_{H\text{-}L}$, and their HOMO energies are close (from -4.76 eV to -5.58 eV). The $\Delta E_{H\text{-}L}$ of pyrene derivatives are remarkably larger than those of PDI derivatives, for instance, molecule **5-1** (3.31 eV)>**1-**

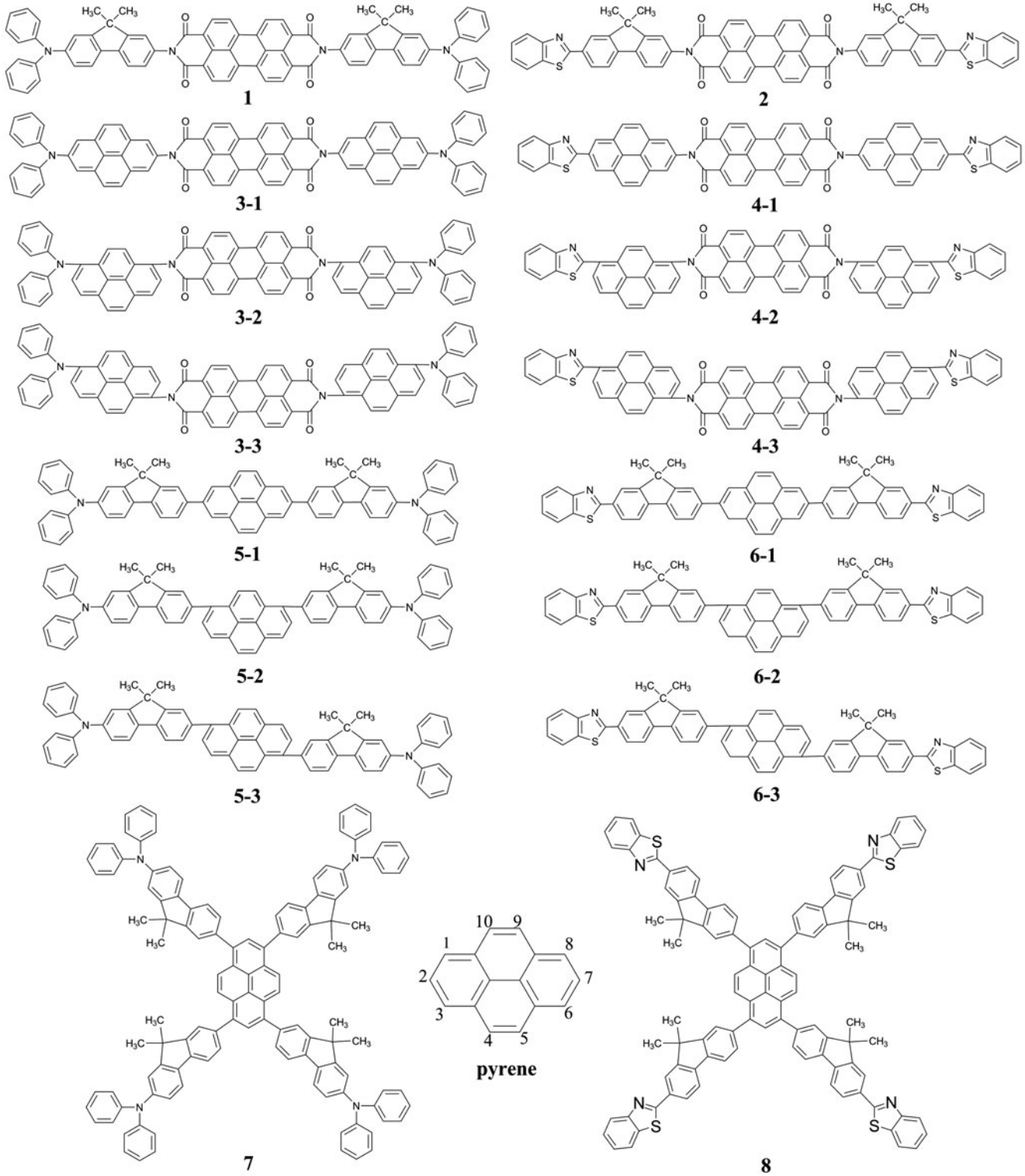

Fig. 2 Molecular structures of the studied compounds

trans (1.49 eV). For PDI derivatives, the $\Delta E_{\text{H-L}}$ of molecules capped with benzothiazole substituents are larger than the ones with diphenylamino groups, such as **2-trans** (2.24 eV) > **1-trans** (1.49 eV), **4-1** (2.09 eV)>**3-1** (1.61 eV), **6-1** (3.58 eV)>**5-1** (3.31 eV), **8** (2.98 eV)>**7** (2.97 eV) and so forth. For compounds **3-1**, **3-2** and **3-3**, the $\Delta E_{\text{H-L}}$ are in the order **3-1** (1.61 eV)>**3-2** (1.51 eV) > **3-3** (1.50 eV), and the same order for the series of

compounds **4**. But when pyrene is taken as the center with different substituents at 2,7-, 1,6-, and 1,8-positions, the order of $\Delta E_{H\text{-}L}$ is **5-1** (3.31 eV)>**5-3** (3.15 eV) > **5-2** (3.14 eV), **6-1** (3.58 eV)>**6-3** (3.24 eV) > **6-2** (3.22 eV). That is to say, the $\Delta E_{H\text{-}L}$ of the molecules bearing 2,7-disustituted pyrene as the π-conjugated bridge or center is larger than that of any other isomers. As illustrated (Fig. 3), the HOMO energy increases and the LUMO energy decreases, then the $\Delta E_{H\text{-}L}$ decreases with the number of fluorene terminal groups increasing.

From the molecular ground-state energy (see Fig. S1) and energy gap analysis above, we can draw a conclusion that molecules **5-1** and **6-1** have both the thermal and dynamic stability with respect to **5-2**, **5-3**, **6-2** and **6-3**.

One-photon absorption properties

The OPA properties of all the investigated molecules were calculated by employing the ZINDO program on the basis of the optimized geometric structures. The TDDFT//B3LYP/6-31G* method was also used to study the OPA properties for the sake of comparison. In addition, the effect of solvent was taken into account by performing B3LYP/6-31G* calculations. The ZINDO calculated maximum OPA wavelengths (λ^{O}_{max}), corresponding oscillator strengths (f), and transition nature are listed in Table 1, and TDDFT calculated values and some experimental data are also summarized in Table 1. In comparison with the results, the λ^{O}_{max} values of molecules **1** and **2** obtained by both TDDFT (530.8 and 531.8 nm, in toluene) and ZINDO (529.3 and 531.8 nm) methods are in good agreement with the experimental values (528±1 and 529±1 nm). Therefore, the ZINDO method is appropriate for the studied molecules in this work. For molecules **1** and **2**, the one-photon absorption properties of both their *trans*- and *cis*-isomers were calculated and the results clearly show that the *trans*- and *cis*- isomers have almost the same OPA properties. Therefore we will use the *trans*–form in the following discussion.

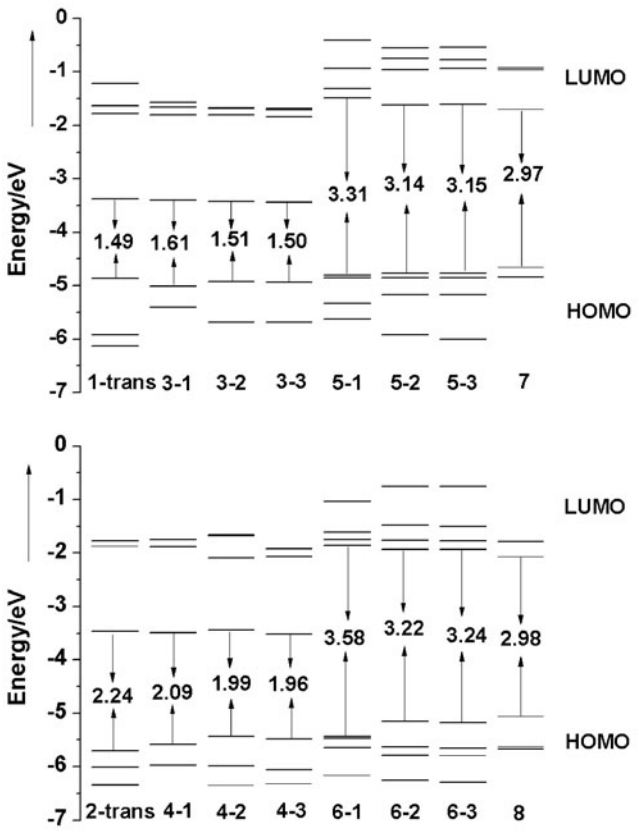

Fig. 3 Calculated frontier orbital energy levels by the B3LYP/6-31G* method

As clearly shown in Table 1, the λ^{O}_{max} values of molecules with the PDI center are on the order of 530 nm which is very close to isolated perylene diimide (λ^{O}_{max}= 526 nm) [22] except molecule **4-2** (502.4 nm) with a hypsochromic shift. Molecules **3-1** and **4-1** with respect to other compounds have much larger oscillator strengths (2.67, 2.07) in the mid-energy absorption band. For molecules **1**, **2**, **4-1**, and **4-2**, the main absorption is from the transition of HOMO-4→LUMO in the low-energy region but for the series of molecules **3** and molecule **4-3**, it is mainly due to the transition of HOMO-6→LUMO. In order to confirm the transition nature, contour surfaces of the frontier molecular orbitals (FMO) relevant to the maximal OPA for the studied molecules are depicted (Fig. 4 and Fig. S2). It can be found that the LUMOs locate on the PDI center no matter whether the terminal substituents are electron-deficient or electron-rich, or the π-conjugated bridges are fluorene or pyrene. So the low-energy absorption band of the PDI derivatives is determined by the perylene ring. But the high-energy absorption band is more complicated and affected by peripheral groups.

The λ^{O}_{max} values of the pyrene compounds (**5** and **6**) are significantly blue-shifted by 93-128 nm compared to PDI molecules **1** and **2**. This trend is just corresponding to the larger $\Delta E_{H\text{-}L}$ of **5** and **6** above. When the $\Delta E_{H\text{-}L}$ of compounds **5-1**, **5-3** and **5-2** decrease in sequence, the λ^{O}_{max} values exhibit bathochromic-shifts (401.8 nm, 427.6 nm and 433.8 nm). When the terminal groups are replaced by benzothiazole, the series of molecules **6** also follow the same trend. With the number of branches increasing, the main absorption in the low-energy region for cruciforms **7** and **8** is composed of the transition of HOMO→LUMO. It is clearly found that significant intramolecular charger-transfers are between the pyrene center and four fluorene terminal groups (see Fig. 4 and Fig. S2). Therefore their maximum OPA peaks are red-shifted by 60-70 nm from those of the corresponding

Table 1 One-photon absorption properties

Molecules	λ^{O}_{max}(nm)		f	Transition nature	
	TDDFT	ZINDO			
1-trans	513.0	529.3	1.15	$S_0 \rightarrow S_1$ (H-4)→(L)92%	
	530.8[a]	(528±1)[b]			
	357.4	400.9	1.11	$S_0 \rightarrow S_{20}$ (H-1)→(L+6)32%	(H)→(L+7)30%
		289.0	1.73	$S_0 \rightarrow S_{54}$ (H-17)→(L+3)22%	(H-18)→(L+4)21%
1-cis	513.1	529.3	1.15	$S_0 \rightarrow S_1$ (H-4)→(L)92%	
	357.9	400.8	1.04	$S_0 \rightarrow S_{20}$ (H-1)→(L+7)32%	(H)→(L+6)30%
		288.9	1.75	$S_0 \rightarrow S_{54}$ (H-17)→(L+3)22%	(H-18)→(L+4)23%
2-trans	513.1	531.8	1.36	$S_0 \rightarrow S_1$ (H-4)→(L)90%	
	531.8[a]	(529±1) [b]			
	345.2	449.4	1.11	$S_0 \rightarrow S_9$ (H)→(L+5)29%	(H-1)→(L+6)29%
		288.8	0.98	$S_0 \rightarrow S_{52}$ (H-13)→(L+3)32%	(H-14)→(L+4)31%
2-cis	513.1	531.9	1.36	$S_0 \rightarrow S_1$ (H-4)→(L)90%	
	345.3	449.5	0.93	$S_0 \rightarrow S_9$ (H)→(L+5)17%	(H-1)→(L+5)17%
				(H)→(L+5)12%	(H-1)→(L+6)12%
		288.8	0.98	$S_0 \rightarrow S_{52}$ (H-13)→(L+3)32%	(H-14)→(L+4)31%
3-1	512.9	530.7	1.32	$S_0 \rightarrow S_3$ (H-6)→(L)92%	
		376.9	2.67	$S_0 \rightarrow S_{24}$ (H-2)→(L+9)13%	(H-3)→(L+8)12%
				(H-2)→(L+8)11%	(H-3)→(L+9)11%
		346.2	1.12	$S_0 \rightarrow S_{36}$ (H)→(L+9)16%	(H-1)→(L+8)16%
				(H-3)→(L+5)15%	(H-2)→(L+6)14%
3-2	516.4	532.9	1.15	$S_0 \rightarrow S_5$ (H-6)→(L)87%	
		339.1	1.06	$S_0 \rightarrow S_{44}$ (H-4)→(L+5)14%	(H-5)→(L+6)14%
				(H)→(L+9)13%	(H-1)→(L+8)13%
3-3	516.5	533.2	1.36	$S_0 \rightarrow S_5$ (H-6)→(L)88%	
		338.1	1.13	$S_0 \rightarrow S_{45}$ (H-4)→(L+5)22%	(H-5)→(L+6)22%
				(H)→(L+9)12%	(H-1)→(L+8)11%
4-1	513.2	524.7	1.50	$S_0 \rightarrow S_3$ (H-4)→(L)91%	
		410.8	2.07	$S_0 \rightarrow S_{19}$ (H)→(L+3)16%	(H-1)→(L+4)16%
				(H-2)→(L+7)10%	(H-3)→(L+8)10%
		328.0	1.01	$S_0 \rightarrow S_{38}$ (H-6)→(L+7)19%	(H-5)→(L+8)19%
4-2	516.4	502.4	1.07	$S_0 \rightarrow S_5$ (H-4)→(L)72%	
	395.1	307.5	1.11	$S_0 \rightarrow S_{53}$ (H-2)→(L+8)18%	(H-3)→(L+7)18%
4-3	516.7	530.1	1.61	$S_0 \rightarrow S_5$ (H-6)→(L)78%	
	387.2	319.6	1.50	$S_0 \rightarrow S_{50}$ (H)→(L+20)78%	(H-1)→(L+19)78%
5-1	397.6	401.8	0.95	$S_0 \rightarrow S_4$ (H)→(L+1)14%	
	310.6	258.9	0.97	$S_0 \rightarrow S_{52}$ (H-6)→(L+4)12%	(H-7)→(L+5)11%
5-2	440.1	433.8	0.86	$S_0 \rightarrow S_2$ (H)→(L)68%	
	361.8	375.2	0.96	$S_0 \rightarrow S_{13}$ (H-1)→(L+2)14%	(H)→(L+1)13%
				(H-1)→(L)12%	
5-3	438.6	427.6	1.43	$S_0 \rightarrow S_2$ (H)→(L)65%	
	374.4	366.0	0.97	$S_0 \rightarrow S_{14}$ (H-1)→(L+1)23%	
6-1	386.9	420.6	2.86	$S_0 \rightarrow S_2$ (H-1)→(L)33%	(H-2)→(L+1)34%
6-2	431.8	438.6	1.17	$S_0 \rightarrow S_2$ (H)→(L)55%	(H-1)→(L+1)16%
	366.8	409.1	1.07	$S_0 \rightarrow S_3$ (H-2)→(L+1)23%	(H-1)→(L)16%
				(H-1)→(L+2)14%	(H)→(L+1)11%
6-3	427.0	427.1	2.11	$S_0 \rightarrow S_2$ (H)→(L)52%	(H-1)→(L+1)18%
				(H-2)→(L+2)11%	

Table 1 (continued)

Molecules	λ^{O}_{max}(nm)		f	Transition nature	
	TDDFT	ZINDO			
	342.4	378.6	0.48	$S_0 \rightarrow S_{11}$ (H-1)→(L+1)11%	
7	467.4	487.6	1.17	$S_0 \rightarrow S_2$ (H)→(L)77%	
	377.7	401.7	1.71	$S_0 \rightarrow S_{20}$ (H-1)→(L)11%	
8	465.4	497.1	1.78	$S_0 \rightarrow S_2$ (H)→(L)65%	
	388.6	450.1	1.34	$S_0 \rightarrow S_3$ (H-1)→(L)12%	(H-4)→(L+3)10%
	343.4	447.1	1.13	$S_0 \rightarrow S_4$ (H-2)→(L+2)16%	(H-3)→(L+1)15%

[a] TDDFT with solvent effect

[b] The experimental data in Ref [25]

[c] H denotes the HOMO and L denotes the LUMO

analogues **5-3** and **6-3**. Such large bathochromic shifts indicate a strong electronic coupling between the pyrene center and the four branches. In addition, the λ^{O}_{max} of molecule **8** is shifted bathochromically compared to **7**, which may be attributed to benzothiazole substituents increasing the conjugation length.

Taking into account all of the molecules studied here, the results provide evidence that the OPA properties are predominantly determined by the structure of center moiety and slightly affected by terminal substituents. As shown in Fig. 3, the $\Delta E_{H\text{-}L}$ of the series of molecules **1**, **2**, **3** and **4** are in the range of 1.50~2.24 eV, but 3.14~3.58 eV for two series of pyrene molecules **5** and **6**. This leads to their low-energy absorption peaks locating at 500~540 nm and 400~440 nm for molecules **1~4** and **5~6**, respectively. Substitutions at different positions of pyrene (as the π-conjugated bridge or center) have small influence on OPA properties, but the substitutions at the diagonal position (for molecules **3-1** and **4-1**) cause larger f value. This effect on low-energy absorption peaks is at a most 30 nm shift. But the molecular size has more obvious effect on OPA properties in comparison of the tetra-substituted derivatives and the disubstituted compounds.

Additionally, the calculated λ^{O}_{max} values of the series compounds of **5** and **6** are all located in the UV/Vis region. This indicates that the pyrene derivatives retain good transparency, which is important for optical power limiting applications.

Two-photon absorption properties

In order to provide a clearer comparison for the molecules studied in this work, two-photon absorption spectra in the wavelength range of 450–1100 nm are shown in Fig. 5. The detailed results including maximum TPA wavelength (λ^{T}_{max}), maximum TPA cross-section (δ^{T}_{max}), and transition nature are all collected in Table S1. As shown in Fig. 5a and Table S1, the calculated λ^{T}_{max} and δ^{T}_{max} of molecule **2** (646.4 nm, 2408.4 GM (1 GM=1×10^{-50} $cm^4 s$ $photon^{-1}$ $molecule^{-1}$)) are in very good agreement with the experimental results (640 nm, 2000–2500 GM). However, the δ^{T}_{max} value of compound **1** (1212.0 GM at 663 nm) is smaller than the experimental result (3000–3500 GM at 640 nm). The experimental value was obtained in toluene and CH_2Cl_2 with picosecond open aperture Z-scan methods which might include excited-state absorption and stimulated emission processes [25]. Thus the δ=~3500 GM can be considered as an upper limit for the intrinsic TPA cross-section. However, it should not affect our comparative investigation owing to the systematic error. It can be seen from Fig. 5 that all molecules have multiple TPA peaks. The PDI derivatives show three TPA peaks and the maximum TPA cross sections occur at 642–676 nm. The series of pyrene derivatives **5** and **6** exhibit four TPA peaks and δ^{T}_{max} at 450–480 nm. Additionally, there is an obvious TPA in low–energy region of 520–550 nm for **5** series and 628–650 nm for **6** series. The cruciforms **7** and **8** exhibit largely red-shifted λ^{T}_{max} and significantly enhanced δ^{T}_{max} in comparison to their corresponding disubstituted compounds **5-3** and **6-3**. In particular, molecule **8** possesses the largest δ^{T}_{max} value (5009.9 GM) at the long wavelength (671.6 nm) among all the studied molecules, which is important for the application in two-photon fluorescence labeling.

It is well-known that center moieties, π-electron bridges, intramolecular charge-transfer, effective electronic coupling between branches and the extended conjugation molecular size will be important factors for influencing the TPA properties [45–49]. These important factors will be discussed in detail as follows.

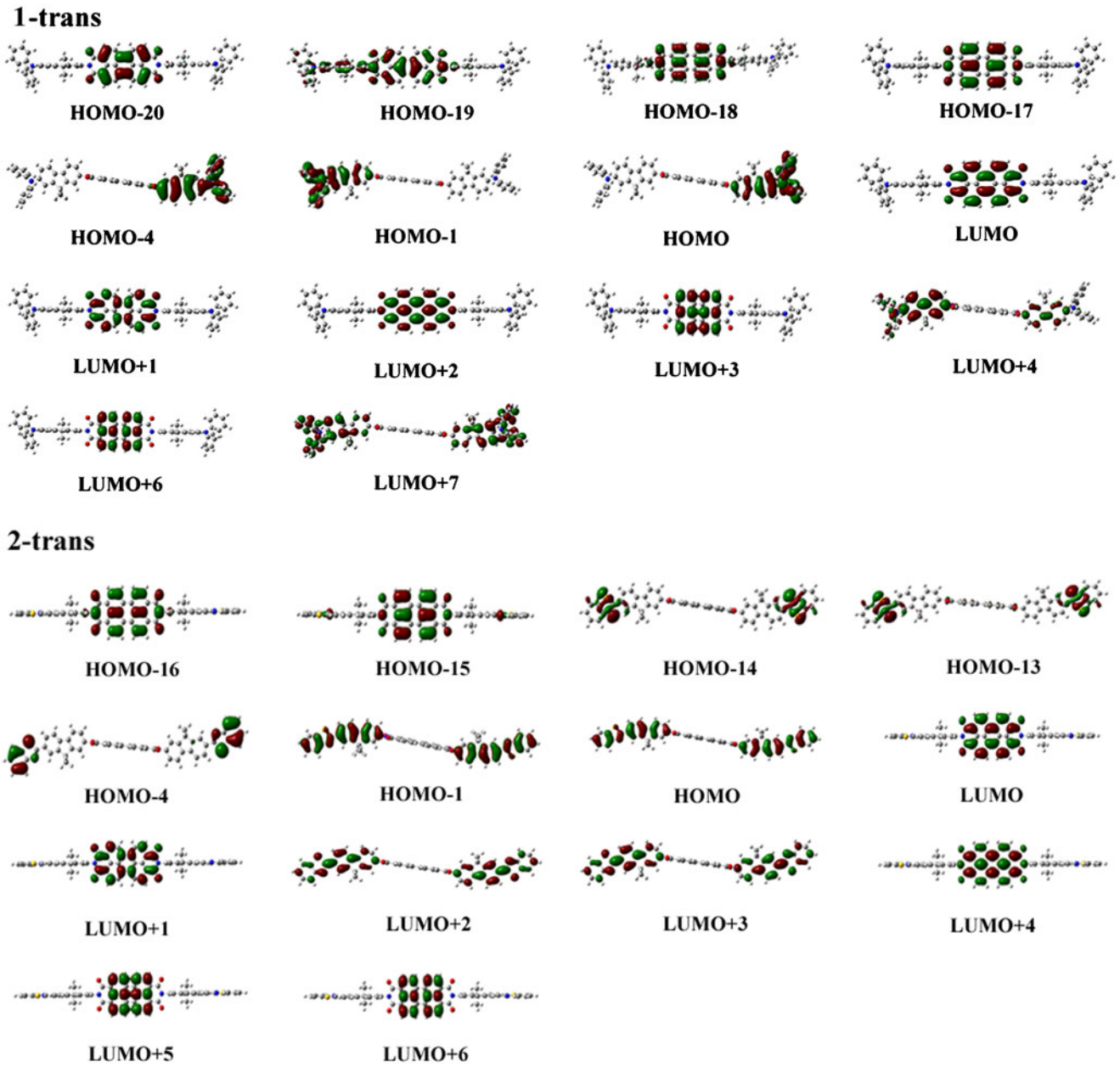

Fig. 4 Contour surfaces of the frontier molecular orbitals relevant to the maximal one- and two-photon absorptions for molecules **1-trans**, **2-trans**, **4-1**, **6-1** and **8**

Effects of center moieties

It can be seen from Figs. 5a, b and c that the TPA spectra of all PDI molecules show a similar shape but different magnitude of δ^{T}_{max}. There are three TPA peaks in the range of 600–1100 nm (the first strong TPA is at 750–1100 nm, the second moderately strong TPA is in the range of 700–750 nm, and the third very strong TPA is in the range of 640–700 nm). The δ^{T}_{max} values of PDI derivatives ranging from 1212.0 to 2418.5 GM at the long wavelength region of 640–800 nm (near infrared region). And in general the organism can endure the light irradiation from near infrared region, so PDI derivatives might be two-photon fluorescence labeling materials for the application in photodynamic therapy.

The series of pyrene molecules **5** and **6** have four TPA peaks, the largest δ^{T}_{max} locate at 450–480 nm and the larger at around 615 nm but at 553 nm for molecules **5-2** and **5-3**. The δ^{T}_{max} values of pyrene derivatives are significantly larger than those of PDI derivatives, especially for molecule **5-2**. The λ^{T}_{max} of pyrene derivatives are blue-shifted relative to PDI derivatives which is attributed to the fact

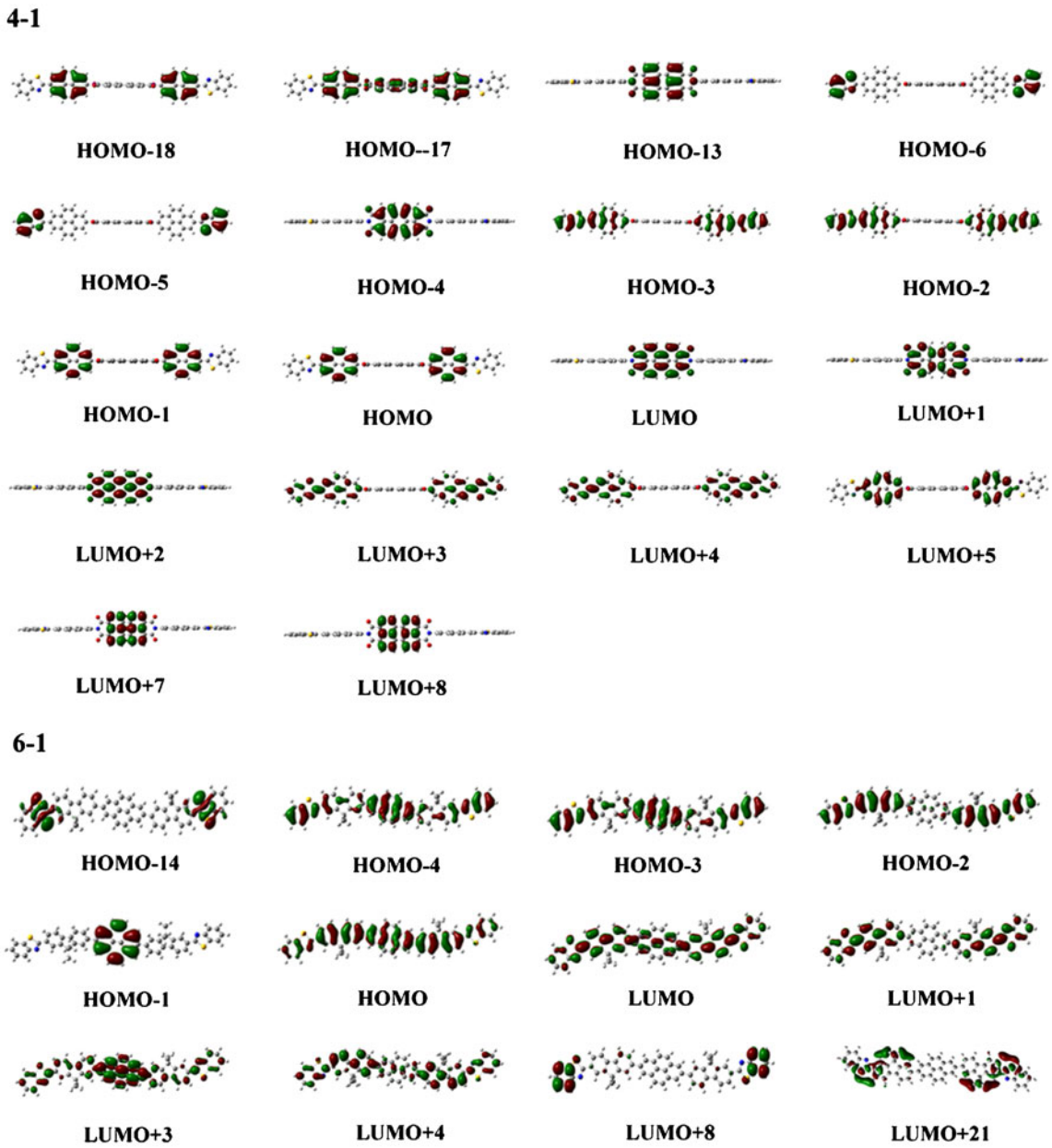

Fig. 4 (continued)

that the TPA final state of pyrene derivatives lies in the higher energy region, such as S_{110} (451.5 nm) for **5-1**. The λ^{T}_{max} of the series of molecules **5** are hypsochromic-shifts by 110–210 nm compared to molecule **1**. While the δ^{T}_{max} values are distinctly increased (from 1212.0 GM to 13669.2 GM) at 400–500 nm, and increased or decreased by 371–160 GM within the range of long wavelengths (500–800 nm). As a whole, compared with molecule **2**, the λ^{T}_{max} values of the series of molecules **6** show hypsochromic-shifts by 150–170 nm and the δ^{T}_{max} values are increased by 1056–8700 GM. But in the range of 500–800 nm, the λ^{T}_{max} are changed slightly (within 20 nm) and the δ^{T}_{max} values are decreased by 108–986 GM. From Figs. 5d and e, it can be seen that 2,7-disubstituted pyrene derivatives (molecules **5-1** and **6-1**) present larger δ^{T}_{max} in the low-energy region than molecules **5-2**, **5-3**, **6-2** and **6-3**.

Effects of π-conjugation bridges

It is interesting to compare the effects of π-conjugation bridges (fluorene and pyrene) on the TPA properties. As shown in Fig. 5b and Table S1, by replacing fluorene as the π-conjugated bridge with pyrene, the δ^{T}_{max} of molecule **3-1** is increased by 145 GM with respect to molecule **1**, while the λ^{T}_{max} remains basically unchanged. And for molecules **3-1**, **3-2** and **3-3** with different substitutions on pyrene (π-

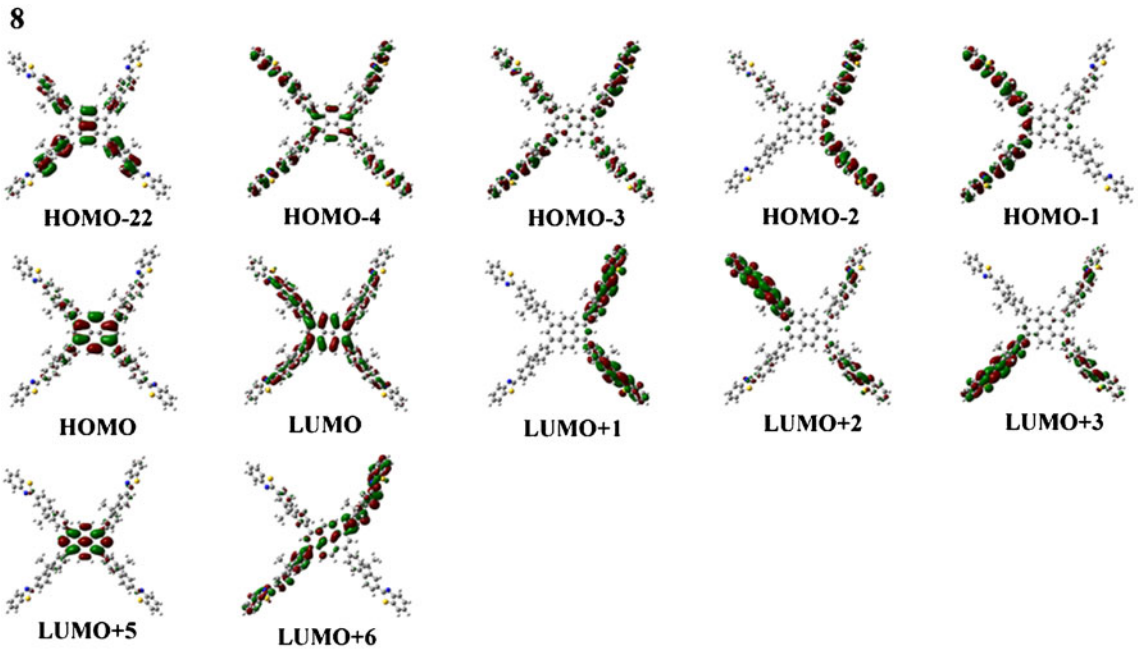

Fig. 4 (continued)

bridge), the maximum TPA cross-sections substantially increase in the order **3-1** (1357.4 GM)<**3-2** (1558.4 GM) < **3-3** (1744.6 GM) at 663.0 nm. But for series of molecules **4**, the λ^{T}_{max} show bathochromic-shifts by 20–30 nm except for molecule **4-2** and the δ^{T}_{max} decrease by ca. 750 GM compared to molecule **2**. With different substitution positions at pyrene bridge, the changing trend of δ^{T}_{max} is **4-1** (1660.6 GM)<**4-2** (1857.6 GM) < **4-3** (2008.0 GM) (see Fig. 5c).

In sum, the different π-conjugation bridges result in the change of TPA cross sections and the different changing trend depends on the coupling interaction between the π-conjugated bridges and terminal groups. Furthermore, it can be concluded that the molecules bearing 1,6-disubstituted pyrene as the π-bridge have larger δ^{T}_{max}.

Effects of substituent terminal groups

The chemical functional groups at the end of molecules are also one of the most important factors on influencing δ^{T}_{max}. As displayed in Table S1 and Fig. 5, the δ^{T}_{max} of molecules with electron-accepting terminal substituents are larger than those of the molecules with electron-donating terminal substituents, that is, **1** (1212.0 GM)<**2** (2408.4 GM), **3-1** (1357.4 GM)<**4-1** (1660.6 GM) and **7** (2532.0 GM)< **8** (5009.9 GM). In the low-energy region of the TPA band, δ^{T}_{max} of the series of compounds **5** are smaller than the corresponding ones of the series of molecules **6**, for instance, **5-1** (1583.5 GM)<**6-1** (2290.1 GM). It is worthy to mention that the δ^{T}_{max} for molecule **2** and cruciform **8** are around 2-fold greater than that of molecules **1** and **7**, respectively. This result can be ascribed to the benzothiazolyl groups stabilizing the planarity of the branch structures, extending the conjugated length, and increasing the π-electron delocalized extent.

Effects of the number of fluorene terminal groups

As reported, the δ^{T}_{max} values of pyrene compounds increased with the number of substituents reaching the maximum value of 1150 GM for the tetra-substituted derivative [32]. Moreover, the cruciforms exhibiting the degree of conjugation, multiple pathways for intramolecular electronic and photonic transfer can enhance δ^{T}_{max} [47].

In the current study, cruciforms **7** and **8** show the largest TPA cross sections at 632.6 nm and 671.6 nm respectively, whereas their λ^{T}_{max} positions are red-shifted by nearly 80 nm and 37 nm from those of the corresponding disubstituent molecules **5-3** (553 nm) and **6-3** (634.5 nm). As shown in Fig. 5f, the most interesting result is that the δ^{T}_{max} value of cruciform **8** (5009.9 GM) is 2.7 times as large as that of molecule **2** (2408.4 GM). It is unexpected that the δ^{T}_{max} value of molecule **7** (2532.0 GM) is two times larger than that of molecule **1** (1212.0 GM). The results still indicate that cruciform **8** with benzothiazolyl terminal groups has the more effective electronic coupling between two adjacent branches, the more extended conjugation length and the more excellent planarity than **7** with four diphenylamine substituents.

Accordingly, the cruciform of pyrene compounds seems to have a certain advantage in enhancing the TPA cross section. And they possess high fluorescence quantum yield

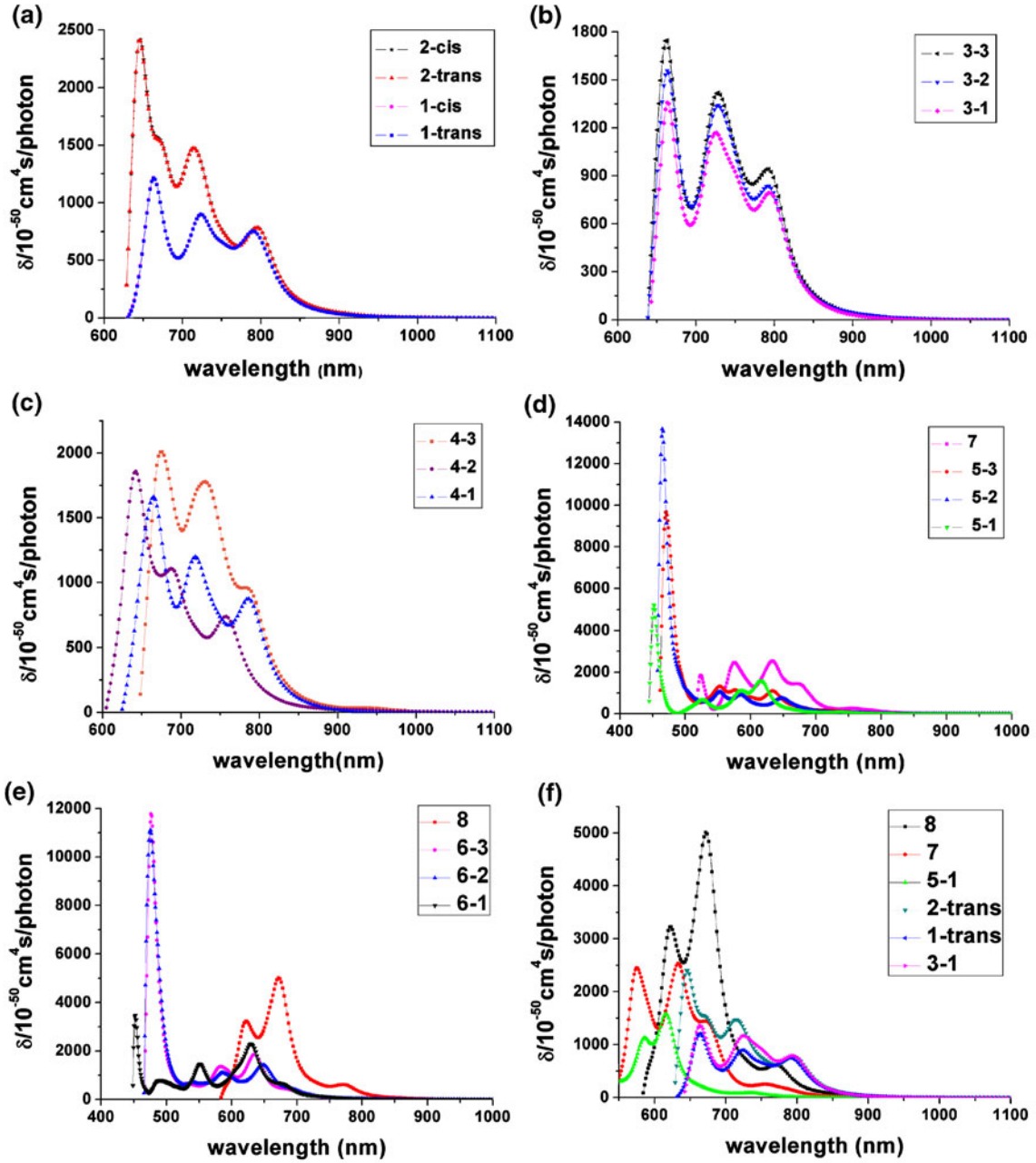

Fig. 5 Two-photon absorption spectra for all molecules

[29, 32]. This suggests that they might be efficient and applicable TPA materials.

Effects of electronic structures

In order to further understand how the frontier molecular orbitals (FMO) can affect TPA properties, we have drawn the molecular orbitals related to main transitions in the two-photon absorption. As shown in Fig. 4, the frontier molecular orbitals of molecules **1**, **2**, **4-1**, **6-1**, and **8** are illustrated. Those of the other studied molecules are shown in Fig. S2. Herein we take molecule **2** as an example to analyze the role of the PDI core and fluorenyl terminal groups in TPA. The maximum TPA at 646.4 nm is composed of the transitions (HOMO-13)→(LUMO+2) 32%, (HOMO-4)→(LUMO+1) 16%, (HOMO-16)→(LUMO+3) 16% and (HOMO-15)→(LUMO) 11%. The transition between HOMO-13 and LUMO+2 is from thiazolyl to lateral sides. But the coefficients of the HOMO-15 are mostly contributed by the center and a little by the thiazolyl and the coefficients of the LUMO are mostly from the PDI moieties. The electron density of the HOMO-16 is delocalized at the PDI core (electron donor), whereas that of the LUMO + 3 is located on both the

fluorenyl and benzothiazolyl moieties. Obviously, the electronic transition between HOMO-16 and LUMO + 3 can be assigned from the center unit to the lateral side groups. The transition between HOMO-4 and LUMO + 1 can be assigned from benzothiazolyl to the PDI center. The electron transitions usually accompany intramolecular charge transfer (ICT). So it is clearly seen that the ICT between the PDI center and the fluorenyl terminal groups is more effective for enhancing two-photon absorption cross-section. By comparing molecule **1** with **2**, in the region of 640–700 nm, there are ICT from one fluorenyl terminal group to the PDI moiety for molecule **1**, but from two benzothiazole substituents to the PDI moiety for molecule **2**. The discrepancy of the intramolecular charge transfers is that both of these benzothiazole groups can efficiently transfer charges to the PDI center through the fluorene groups for **2**. This results in the δ_{max} of molecule **2** is larger than that of **1**. The strongest TPA (at 665.2 nm) of molecule **4-1** comes from electronic excitation $S_0 \rightarrow S_{37}$, which is composed of HOMO-13→LUMO + 2, HOMO-18→LUMO + 5, HOMO-4→LUMO + 1 and HOMO-17→LUMO. The intramolecular charge transfer can be dramatically observed from the pyrene-bridge to the PDI center. For pyrene compounds, taking molecule **6-1** as an example, the strongest TPA (at 452.5 nm) comes from electronic excitation $S_0 \rightarrow S_{96}$, which can be described as the transition of HOMO-1→LUMO+21 corresponding to ICT from the pyrene center to the fluorene and benzothiazolyl moieties. In the region of 600–800 nm, the strong TPA (at 628.7 nm) comes from $S_0 \rightarrow S_{22}$. The configurations of S_{22} are (HOMO-1)→(LUMO+4) 19%, (HOMO-2)→(LUMO+3) 19% and (HOMO-4)→(LUMO+3) 11%, and ICT are assigned from the center moieties, fluorenyl terminal groups or benzothiazolyl parts to the whole molecule. For cruciform **8**, the final state of the strongest TPA (at 671.6 nm) is S_{28} and its main transition is HOMO-3→LUMO, and ICT is from four fluorene terminal groups to the pyrene center. So these multiple pathways for ICT can drastically enhance two-photon absorption cross-sections. The PDI and pyrene derivatives owing to strong intramolecular charge-transfer ability show large δ^{T}_{max} and are expected to be promising TPA materials.

Conclusions

In this present study, the geometric and electronic structures, OPA and TPA properties of pyrene and PDI compounds were comparatively investigated, and the origin of the linear and nonlinear optical properties were further revealed. The calculated results indicate that in comparison with PDI derivatives, the δ^{T}_{max} for the compounds with the pyrene center increase obviously, the maximum OPA and TPA spectra are blue-shifted, and the $\Delta E_{H\text{-}L}$ increase. The different π-conjugated bridges (fluorene and pyrene) and terminal groups have slight effect on OPA properties. Nevertheless, the molecules bearing 1,6-disubstituted pyrene as the π-bridge has the largest δ^{T}_{max} in the series of compounds **3** or **4**. Moreover, the δ^{T}_{max} values of molecules with benzothiazole-substituted terminal groups are larger than those of the molecules with diphenylamine, which is attributed to the benzothiazole groups stabilizing the planarity of the branch parts, extending the conjugated length and increasing the π-electron delocalized extent. Furthermore, the molecular size has a marked effect on OPA and TPA properties. By comparing the tetra-substituted derivatives with the disubstituted compounds, the OPA spectra exhibit red-shifts. Especially, the δ^{T}_{max} of cruciform **8** is 2.7 times as large as that of molecule **6-3** and molecule **8** exhibits the largest TPA cross-section among all the studied molecules in the long spectral regions. It is concluded that the cruciform molecules having considerable degree of conjugation, multiple pathways for intramolecular electronic transfer can largely enhance δ^{T}_{max}.

In conclusion, these derivatives present large TPA cross sections and specific photophysical and photochemical properties which are promising candidates for TPA materials.

Acknowledgments This work is supported by the Natural Science Foundation of China (No. 20973078 and 20673045) as well as the Open Project of the State Key Laboratory for Superamolecular Structure and Material of Jilin University (SKLSSM200716).

References

1. Göppert-Mayer M (1931) Annu Phys 401:273–294
2. Kaiser W, Garrett CGB (1961) Phys Rev Lett 7:229–231
3. Zipfel WR, Williams RM, Webb WW (2003) Nat Biotechnol 21:1369–1377
4. Helmchen F, Denk W (2005) Nat Methods 2:932–940
5. LaFratta CN, Fourkas JT, Baldacchini T, Farrer RA (2007) Angew Chem 119:6352–6374, (2007) Angew Chem Int Ed 46:6238–6258
6. Parthenopoulos DA, Rentzepis PM (1989) Science 245:843–845
7. Cumpston BH, Ananthavel SP, Barlow S, Dyer DL, Ehrlich JE, Erskine LL, Heikal AA, Kuebler SM, Lee IYS, McCord-Maughon D, Qin JQ, Rockel H, Rumi M, Wu XL, Marder SR, Perry JW (1999) Nature 398:51–54
8. Kawata S, Kawata Y (2000) Chem Rev 100:1777–1788
9. Spangler CW (1999) J Mater Chem 9:2013–2020
10. Calvete M, Yang GY, Hanack M (2004) Synth Met 141:231–243
11. Lin TC, Chung SJ, Kim KS, Wang X, He GS, Swiatkiewicz J, Pudavar HE, Prasad PN (2003) Adv Polym Sci 161:157–193
12. Fisher WG, Partridge WP Jr, Dees C, Wachter EA (1997) Photochem Photobiol 66:141–155
13. Velusamy M, Shen JY, Lin JT, Lin YC, Hsieh CC, Lai CH, Lai CW, Ho ML, Chen YC, Chou PT, Hsiao JK (2009) Adv Funct Mater 19:2388–2397
14. Shibano Y, Imahori H, Adachi C (2009) J Phys Chem C 113:15454–15466

15. Chen XQ, Jou MJ, Yoon J (2009) Org Lett 11:2181–2184
16. Kohl C, Weil T, Qu J, Müellen K (2004) Chem Eur J 10:5297–5310
17. Chen HZ, Ling MM, Mo X, Shi MM, Wang M, Bao Z (2007) Chem Mater 19:816–824
18. Jones BA, Fachetti A, Wasielewski MR, Marks TJ (2008) Adv Funct Mater 18:1329–1339
19. Shin WS, Jeong HH, Kim MK, Jin SH, Kim MR, Lee JK, Lee JW, Gal YS (2006) J Mater Chem 16:384–390
20. De Boni L, Constantino CJL, Misoguti L, Aroca RF, Zilio SC, Mendonca CR (2003) Chem Phys Lett 371:744–749
21. Oliveira SL, Corrêa DS, Misoguti L, Constantino CJL, Aroca RF, Zilio SC, Mendonca CR (2005) Adv Mater 17:1890–1893
22. Corrêa DS, Oliveira SL, Misoguti L, Zilio SC, Aroca RF, Constantino CJL, Mendonca CR (2006) J Phys Chem A 110:6433–6438
23. Zhao Y, Ren AM, Feng JK, Sun CC (2008) J Chem Phys 129:014301–1
24. Belfield KD, Schafer KJ, Alexander MD (2000) Chem Mater 12:1184–1186
25. Belfield KD, Bondar MV, Hernandez FE, Przhonska OV (2008) J Phys Chem C 112:5618–5622
26. Belfield KD, Bondar MV, Przhonska OV, Schafer KJ (2002) J Photochem Photobiol A Chem 151:7–11
27. Law KY (1993) Chem Rev 93:449–486
28. Smalley MK, Silverman SK (2006) Nucleic Acids Res 34:152–166
29. Ji SM, Yang J, Yang Q, Liu SS, Chen MD, Zhao JZ (2009) J Org Chem 74:4855–4865
30. Maeda H, Maeda T, Mizuno K, Fujimoto K, Shimizu H, Inouye M (2006) Chem Eur J 12:824–831
31. Wee KR, Ahn HC, Son HJ, Han WS, Kim JE, Cho DW, Kang SO (2009) J Org Chem 74:8472–8475
32. Kim HM, Lee YO, Lim CS, Kim JS, Cho BR (2008) J Org Chem 73:5127–5130
33. Becke AD (1993) J Chem Phys 98:5648
34. Becke AD (1988) Phys Rev A 38:3098–3100
35. Lee C, Yang W, Parr RG (1988) Phys Rev B 37:785–789
36. Frisch MJ, Trucks GW, Schlegel HB, Scuseria GE, Robb MA, Cheeseman JR, Montgomery JA, Vreven T, Kudin KN, Burant JC, Millam JM, Iyengar SS, Tomasi J, Barone V, Mennucci B, Cossi M, Scalmani G, Rega N, Petersson GA, Nakatsuji H, Hada M, Ehara M, Toyota K, Fukuda R, Hasegawa J, Ishida M, Nakajima T, Honda Y, Kitao O, Nakai H, Klene M, Li X, Knox JE, Hratchian HP, Cross JB, Bakken V, Adamo C, Jaramillo J, Gomperts R, Stratmann RE, Yazyev O, Austin AJ, Cammi R, Pomelli C, Ochterski JW, Ayala PY, Morokuma K, Voth GA, Salvador P, Dannenberg JJ, Zakrzewski VG, Dapprich S, Daniels AD, Strain MC, Farkas O, Malick DK, Rabuck AD, Raghavachari K, Foresman JB, Ortiz JV, Cui Q, Baboul AG, Clifford S, Cioslowski J, Stefanov BB, Liu G, Liashenko A, Piskorz P, Komaromi I, Martin RL, Fox DJ, Keith T, Al-Laham MA, Peng CY, Nanayakkara A, Challacombe M, Gill PMW, Johnson B, Chen W, Wong MW, Gonzalez C, Pople JA (2004) Gaussian 03, revision C.02. Gaussian, Wallingford CT
37. Cances E, Mennucci B, Tomasi J (1997) J Chem Phys 107:3032–3041
38. Cossi M, Barone V, Cammi R, Tomasi J (1996) Chem Phys Lett 225:327–335
39. Miertus S, Tomasi J (1982) Chem Phys 65:239–245
40. Miertus S, Scrocco E, Tomasi J (1981) Chem Phys 55:117–129
41. Cha M, Torruellas WE, Stegeman GI, Horsthuis WHG, Möhlmann GR, Meth J (1994) Appl Phys Lett 65:2648–2650
42. Kogej T, Beljonne D, Meyers F, Perry JW, Marder SR, Brédas JL (1998) Chem Phys Lett 298:1–3
43. Orr BJ, Ward JF (1971) Mol Phys 20:513–526
44. Bishop DM, Luis JM, Kirtman B (2002) J Chem Phys 116:9729–9379
45. Beljonne D, Wenseleers W, Zojer E, Shuai Z, Vogel H, Pond SJK, Perry JW, Marder SR, Brédas JL (2002) Adv Funct Mater 12:631–641
46. Albota M, Beljonne D, Brédas JL, Ehrlich JE, Fu JY, Heikal AA, Hess SE, Kogej T, Levin MD, Marder SR, McCord-Maughor D, Perry JW, Röckel H, Rumi M, Subramaniam G, Webb WW, Wu XL, Xu C (1998) Science 281:1653–1656
47. Zhang HC, Guo EQ, Zhang YL, Ren PH, Yang WJ (2009) Chem Mater 21:5125–5135
48. Òscar RP, Luo Y, Ågren H (2006) J Chem Phys 124:094310–094311
49. Ma WB, Wu YQ, Gu DH, Gan FX (2006) J Mol Struct THEOCHEM 772:81–87